

REPORT



## Agonistic nanobodies and antibodies to human VISTA

Yu-Heng Vivian Ma<sup>a,\*</sup>, Amanda Sparkes<sup>a,\*</sup>, Ema Romão<sup>b</sup>, Shrayasee Saha<sup>c</sup>, and Jean Gariépy<sup>a,c,d</sup>

<sup>a</sup>Physical Sciences, Sunnybrook Research Institute, Toronto, Canada; <sup>b</sup>Cellular and Molecular Immunology Lab, Vrije Universiteit Brussel, Ixelles, Belgium; <sup>c</sup>Department of Pharmaceutical Sciences, University of Toronto, Toronto, Canada; <sup>d</sup>Department of Medical Biophysics, University of Toronto, Toronto, Canada

### ABSTRACT

The V-domain Ig Suppressor of T-cell Activation (VISTA) is an immune checkpoint regulator that suppresses immune responses and is readily expressed on human and murine myeloid cells and T cells. This immunosuppressive pathway can be activated using VISTA agonists. Here, we report the development of murine anti-human VISTA (anti-hVISTA) monoclonal antibodies (mAbs), anti-hVISTA nanobodies (Nbs), and cross-reactive rat anti-murine/human VISTA (anti-hmVISTA) mAbs. All mAbs and Nbs generated bound to VISTA (human and/or murine) with dissociation constants in the sub-nanomolar or low nanomolar range. Competition analysis revealed that the selected Nbs bound the same or a nearby epitope(s) as the human VISTA-specific mAbs. However, the cross-reactive mAbs only partially competed with Nbs for binding to hVISTA. All mAbs and one Nb (hVISTANb7) were able to strongly detect VISTA expression on primary human monocytes. Importantly, the murine anti-hVISTA mAbs 7E12 and 7G5 displayed strong agonistic activity in human peripheral blood mononuclear cell cultures, while Nb7 and rat anti-hmVISTA mAbs 3C3, 7C6, 7C7, and 7G1 also behaved as hVISTA agonists, albeit to a lesser extent. Cross-reactive mAbs 7C7 and 7G1 further displayed agonistic potential in murine splenocyte assays. Importantly, mAb 7G1 significantly reduced inflammation associated with the murine model of imiquimod-induced psoriasis. These agonistic VISTA mAbs may represent therapeutic leads to treat inflammatory disorders.

### ARTICLE HISTORY

Received 21 June 2021  
Revised 22 October 2021  
Accepted 2 November 2021

### KEYWORDS

VISTA; monoclonal antibodies; nanobodies; agonistic; anti-inflammatory; psoriasis; ConA

## Introduction

The immune system is regulated by a series of co-stimulatory and co-inhibitory signals. This delicate balance allows the immune system to protect against pathogens while preserving self-tolerance. Engagement of co-inhibitory [immune checkpoint] pathways involving PD-1:PD-L1 and CTLA-4:CD80/CD86 receptor-ligand pairs lead to T-cell suppression. Biologics that inhibit these immune checkpoint pathways have proven to be very effective in cancer immunotherapy,<sup>1</sup> while checkpoint agonists that activate these immune checkpoint pathways could be applied to treat autoimmune diseases or suppress inflammation.

V-domain immunoglobulin suppressor of T-cell activation (VISTA) is a recently discovered immune checkpoint that bears sequence homology to PD-L1. VISTA is expressed predominantly on the surface of hematopoietic cells, with the highest level of expression found on myeloid cells.<sup>2,3</sup> Interestingly, VISTA has been proposed to function both as a ligand and as a receptor, as both exogenous VISTA<sup>2-6</sup> and agonistic anti-VISTA antibodies<sup>7-9</sup> suppress T-cell functions. Considerable effort has gone into generating antibodies that block the function of VISTA in the context of cancer immunotherapy. However, VISTA is an attractive therapeutic target for treating inflammatory disorders as well since VISTA-deficient mice display a higher basal level of immune activation<sup>10</sup>



and are more sensitive to developing ConA-induced hepatitis,<sup>8</sup> encephalomyelitis,<sup>4</sup> systemic lupus erythematosus,<sup>11</sup> asthma,<sup>12</sup> lupus erythematosus,<sup>13</sup> and exacerbated imiquimod (IMQ)-induced psoriasiform inflammation of the ear.<sup>6</sup>

Here, we describe the generation of a new repertoire of agonistic anti-human VISTA (anti-hVISTA) monoclonal antibodies (mAbs) and nanobodies (Nbs) and demonstrate their functional activities. In particular, two human-specific mAbs 7E12 and 7G5 exhibited strong agonistic properties in suppressing ConA-induced activation of human T cells in whole peripheral blood mononuclear cell (PBMC) cultures. *In vivo* use of the cross-species anti-human/murine VISTA (anti-hmVISTA) mAb clone 7G1 in an IMQ-induced murine model of psoriasis exemplifies the therapeutic potential of agonizing VISTA for the treatment of inflammatory disorders.


## Results

### Characterization of anti-VISTA mAbs and Nbs

Following ELISA screenings against human and mouse VISTA (hVISTA and mVISTA), five hybridoma clones generating murine anti-hVISTA mAbs (7G5, 7E12, 10B5, 5F2, and 8G10) and five hybridoma clones generating rat anti-hmVISTA mAbs (3C3, 7C6, 7C7, 7G1, and 11A1) were selected and further expanded based on their production levels.

**CONTACT** Jean Gariépy  [jean.gariepy@utoronto.ca](mailto:jean.gariepy@utoronto.ca)  Physical Sciences, Sunnybrook Research Institute, 2075 Bayview Ave., Room M7-434, Toronto, ON M4N 3M5, Canada

\*These authors contributed equally to this work.

 Supplemental data for this article can be accessed on the [publisher's website](#).

© 2021 The Author(s). Published with license by Taylor & Francis Group, LLC.

This is an Open Access article distributed under the terms of the Creative Commons Attribution-NonCommercial License (<http://creativecommons.org/licenses/by-nc/4.0/>), which permits unrestricted non-commercial use, distribution, and reproduction in any medium, provided the original work is properly cited.

All of the selected murine clones generated mouse IgG1 anti-hVISTA mAbs. The variable regions of the five chosen clones were sequenced and pooled into three different families based on similarities in their heavy chain complementarity-determining region 3 (CDR3) (Figure 1a), a region typically associated with mAb specificity.<sup>14</sup> The presence of heavy and light chains as well as the purity of mAbs were confirmed by SDS-PAGE and by Western blot detected using an anti-mouse IgG heavy and light chain antibody (Figure 1b).

Representative mAbs from each of the three families, namely 7E12, 7G5, and 8G10, were chosen for further characterization based on their sub-nanomolar binding (equilibrium dissociation constant;  $K_D$ ) to human VISTA ( $K_D$  values of 0.44 nM, 0.14 nM, and 0.98 nM, respectively) as measured by surface plasmon resonance (SPR) (Figure 2a). As expected, none of these murine antibodies recognized recombinant mouse VISTA (Supplementary Figure s1). In

addition to the murine anti-hVISTA clones, five rat hybridoma clones were selected based on their production of mAbs that bind to both human and murine VISTA. All five clones produce mAbs (Figure 1b) of the rat IgG2a subtype. As sequencing shows that two of the rat mAbs (7C6 and 11A1) have the same heavy chain sequence, four hybridoma clones were selected for further characterization (3C3, 7C6, 7C7, and 7G1) (Figure 1a). All of the selected clones bound to both hVISTA ( $K_D$  values of 0.24 nM, 840 nM, 49 nM, and 44 nM, respectively; Figure 2b) and mVISTA ( $K_D$  values of 1.3 pM, 3 nM, 51 nM, and 6.7 nM, respectively; Figure 2c).

In addition to the mAbs, seven positive anti-hVISTA Nbs phage clones (hVISTANb1 to 7; Nb1 to Nb7) were identified from bio-panning against hVISTA. The seven anti-hVISTA Nbs phage clones identified were regrouped into three families based on amino acid sequence differences within their CDR domains (Figure 1a). One clone corresponding to each of the

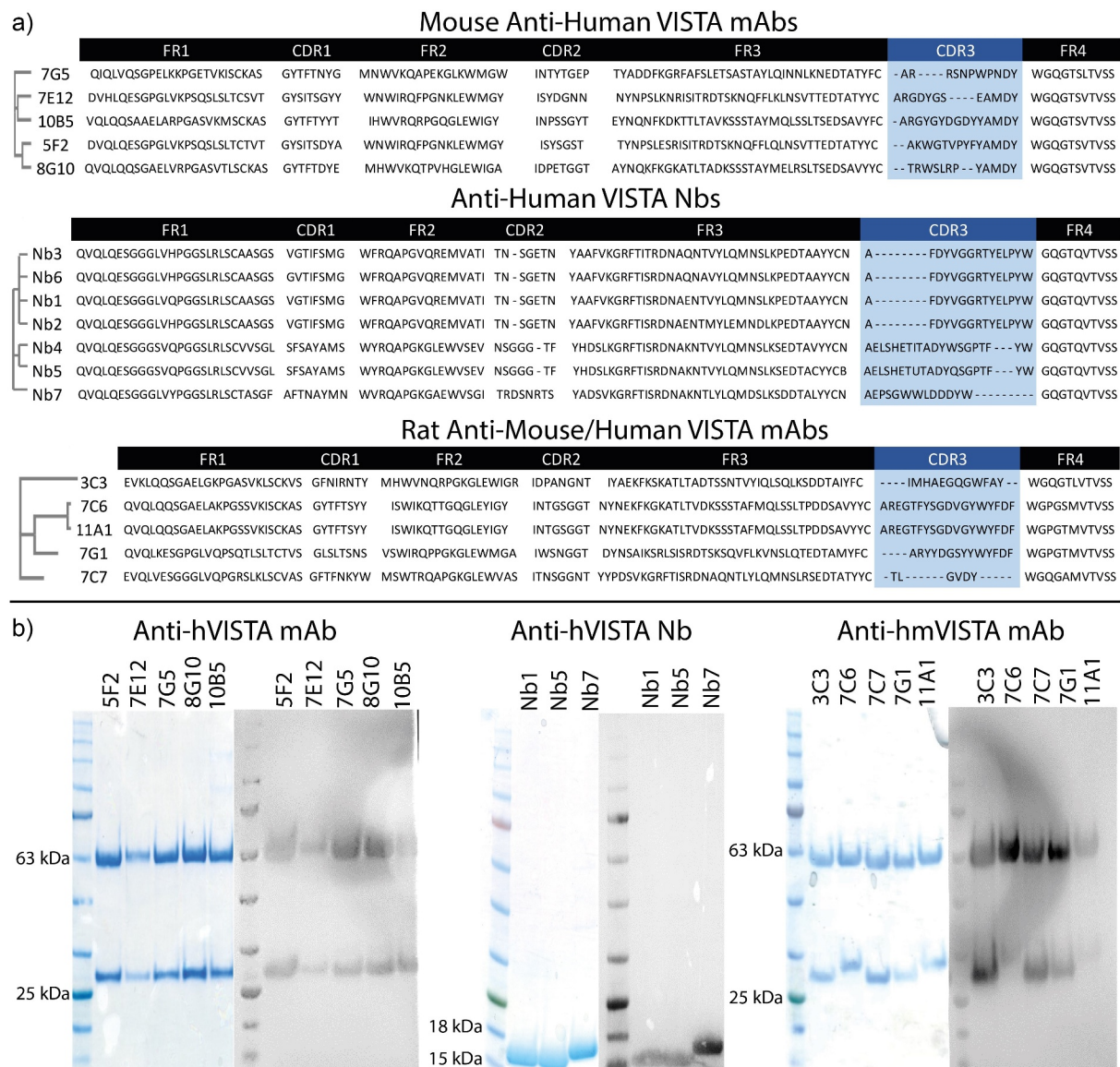


**Figure 1.** Sequence alignment and production of anti-VISTA mAbs and Nbs. (a) Sequence alignments of the variable regions of heavy chains of mouse anti-hVISTA mAbs, anti-hVISTA Nbs, and rat anti-hmVISTA mAbs, clustered based on sequence similarity of CDR3. (b) SDS-PAGE gel and Western blot of anti-VISTA mAbs and Nbs under reducing conditions. Bands on Western blots were detected using an antibody conjugated to HRP that recognizes heavy and light chains of mouse or rat IgGs.

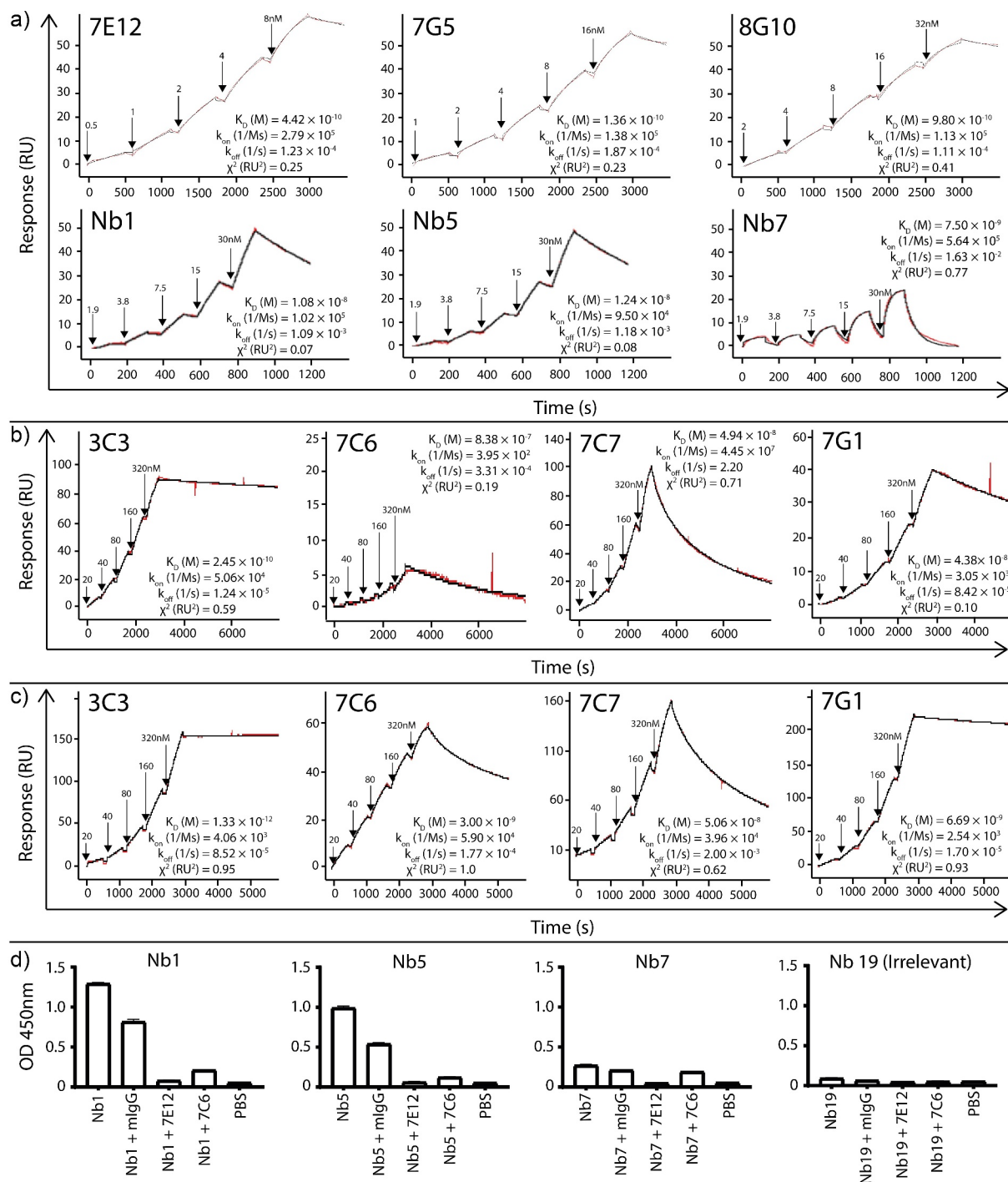


**Figure 2.** Binding of mAbs and Nbs to VISTA. (a-c) SPR single-cycle kinetics sensorgrams (in red) and fitted curves (in black) with equilibrium ( $K_D$ ), association ( $k_{on}$ ) and dissociation ( $k_{off}$ ) rate constants depicting the binding of (a) mouse anti-hVISTA mAbs (7E12, 7G5, 8G10) and anti-hVISTA Nbs (Nb1, Nb5, Nb7) to human VISTA, (b) rat anti-hmVISTA mAbs (3C3, 7C6, 7C7, 7G1) to human VISTA, and (c) rat anti-hmVISTA mAbs to mouse VISTA. (d) Competition ELISA of anti-hVISTA Nbs, or an irrelevant control Nb19, with representative anti-hVISTA (7E12) or anti-hmVISTA (7C6) mAbs ( $n = 3$ ).

families, termed Nb1, Nb5, and Nb7, was chosen for production and characterization. All three Nbs were successfully purified as evidenced by the expected molecular weight band (~15 kDa) on SDS-PAGE and by Western blot (Figure 1b). Nb1, Nb5, and Nb7 bound to hVISTA with  $K_D$  in the low nM range (11 nM, 12 nM, and 7.5 nM, respectively) as determined by SPR (Figure 2a). None of the Nbs recognized mVISTA (Supplementary Figure s1). All binding parameters are summarized in Supplementary Table 1.

To further confirm the selectivity and specificity of the Nbs for hVISTA, a competition ELISA was performed to assess the ability of selected mAbs to displace the binding of Nbs to hVISTA. Figure 2d shows that 2-fold molar excess of the representative anti-hVISTA mAb 7E12, but not the control mouse IgG1, was able to fully displace Nb1, Nb5, and Nb7 from binding to hVISTA. A representative epitope binning on SPR using 7E12 in competition with Nb1 corroborated these results (Supplementary Figure 2). Specifically, hVISTA-Fc

bound to Nb1 immobilized on the chip is displaced in the presence of mAb 7E12. The irrelevant control Nb19 did not bind hVISTA. Notably, a representative of the cross-reactive anti-hmVISTA family, mAb 7C6, only partially displaced the Nbs from binding to hVISTA, suggesting that the cross-reactive mAb binds a partly distinct epitope from the mAbs that bind specifically to human VISTA. As confirmed by SPR and notwithstanding steric hindrance, all human-specific mAbs bound to the same or overlapping epitope, whereas the cross-reactive mAbs, represented by 3C3, bound an alternative epitope (Supplementary Figure 2).

In addition to SPR and ELISA analyses, we further assessed the binding specificity of the mAbs and Nbs to the surface of HEK cells (Expi293F) transiently transfected to express human VISTA on the cell surface. Expression of hVISTA was confirmed using a commercially available positive control mAb (clone B7H5DS8; eBioscience). As shown in Figure 3a, the reagents tested, with the exception of mAb 7C7, were able to detect hVISTA expression on the transfected cells, but not the non-transfected cells.

### mAbs optimally detect VISTA on primary human and murine myeloid cells

VISTA is predominately expressed on cells of the myeloid compartment (monocytes, macrophages, neutrophils, and dendritic cells) and to a lesser extent in naïve CD4<sup>+</sup> and

CD8<sup>+</sup> T cells.<sup>3,4,8</sup> Flow cytometry was thus used to detect the binding of selected mAbs and Nbs to CD14<sup>+</sup>CD16<sup>-</sup> classical monocytes, CD4<sup>+</sup> T cells, and CD8<sup>+</sup> T cells in PBMCs isolated from healthy donors. As shown in Figure 3b, similar to the results obtained on transfected cells, all of the mAbs investigated (anti-hVISTA mAbs 7E12, 7G5, and 8G10 and anti-hmVISTA mAbs 3C3, 7C6, 7C7, and 7G1) detected VISTA expression on human classical monocytes, at a comparable level as the commercially available control mAb (clone B7H5DS8; eBioscience). No binding was detected on either T-cell subset. However, of the anti-hVISTA Nbs, only Nb7 was able to strongly detect VISTA expression on human classical monocytes. As was the case for all mAbs, none of the Nbs detected VISTA expression on T cells. As such, the functional characterization of only the mAbs and Nb7 were subsequently pursued.

Similarly, the cross-species anti-hmVISTA mAbs were tested for their ability to bind immune cell populations in mouse splenocytes. As shown in Figure 3c, all of the mAbs bind mouse macrophages and neutrophils at a comparable level to their binding to human CD14<sup>+</sup>CD16<sup>-</sup> monocytes, although binding for mAb 3C3 was not statistically significant. In contrast to binding on human T cells, the mAbs detected VISTA expression on murine CD4<sup>+</sup> T cells in accordance with previous studies.<sup>3</sup> Notably, mAb 7G1 exhibited the highest binding to both human and murine immune cell populations known to express VISTA.

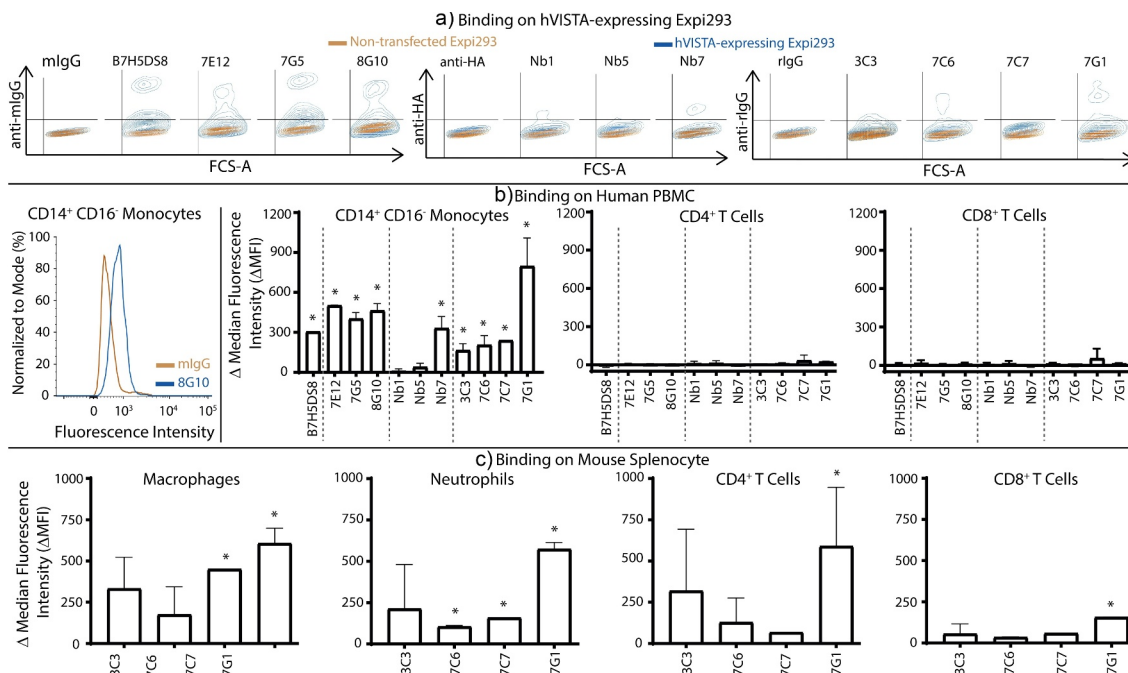


**Figure 3.** Binding of anti-VISTA mAbs and Nbs to Expi293F cells transiently expressing hVISTA and primary immune cell sub-populations present in human PBMCs and mouse splenocytes. (a) Plots depict the binding of a commercial anti-hVISTA antibody (B7H5DS8), anti-hVISTA murine mAbs (7E12, 7G5, 8G10) and Nbs (Nb1, Nb5, Nb7), and anti-hmVISTA rat mAbs (3C3, 7C6, 7C7, 7G1) to Expi293F cells transiently transfected to express hVISTA on the cell surface (orange) in comparison to binding to non-transfected cells (blue). (b) Right panel histograms depict the binding of a commercial anti-hVISTA antibody (B7H5DS8), anti-hVISTA murine mAbs (7E12, 7G5, 8G10) and Nbs (Nb1, Nb5, Nb7), and anti-hmVISTA rat mAbs (3C3, 7C6, 7C7, 7G1) to human CD14<sup>+</sup>CD16<sup>-</sup> monocytes and CD4<sup>+</sup> and CD8<sup>+</sup> T cells from PBMCs of 5 donors (reported as ΔMFI, the difference between MFI values recorded for mAbs or Nb and their respective isotype control). Left panel shows a representative cytometric profile of the binding of murine anti-hVISTA mAb 8G10 to human CD14<sup>+</sup>CD16<sup>-</sup> monocytes relative to its isotype control murine IgG (mIgG), normalized to mode (% of counts in the maximum peak). (c) Histograms depicting the binding of anti-hmVISTA rat mAbs to macrophages, neutrophils, and CD4<sup>+</sup> and CD8<sup>+</sup> T cells from splenocytes of 3 mice (reported as ΔMFI). Data is shown as mean ± SD. \*p < .05 by Student's t-test between MFIs of mAbs or Nbs and their isotype controls.

## Anti-hVISTA mAbs 7E12 and 7G5 display strong agonistic potential

From a functional standpoint, VISTA is described as a negative checkpoint regulator of immune responses. Accordingly, agonizing or antagonizing VISTA is potentially consequential for the treatment of inflammatory conditions or cancer, respectively. *Ex vivo* experiments were thus conducted with human PBMCs to define if anti-hVISTA mAbs 7E12, 7G5, and 8G10, anti-hVISTA Nb7, and anti-hmVISTA mAbs 3C3, 7C6, 7C7, and 7G1 behave as human VISTA agonists or antagonists. Herein, human PBMC cultures were stimulated with concanavalin A (ConA; 1  $\mu\text{g}/\text{mL}$ ) in the presence or absence of a predetermined optimal concentration of mAbs (Supplementary Figure 3) or Nb7. CD4<sup>+</sup> and CD8<sup>+</sup> T-cell proliferation responses (Figure 4) and cytokine levels (Figure 5) were subsequently assessed.

Two of the mAbs, 7E12 and 7G5, strongly inhibited the proliferation of CD4<sup>+</sup> and CD8<sup>+</sup> T cells induced by ConA (Figure 4), caused a reduction in ConA-induced pro-inflammatory cytokine IL-2 production, and led to a significant increase in levels of the anti-inflammatory cytokine IL-10 when compared to ConA alone (Figure 5), suggesting that both these mAbs behave as hVISTA agonists. In particular, 7E12 displayed the greatest reduction in both CD4<sup>+</sup> and CD8<sup>+</sup> T-cell proliferation (65% and 62%, respectively) and may be an ideal candidate for treating human inflammation-associated disease processes. The inhibitory mechanism of these mAbs does not appear to be linked to cytotoxicity (Supplementary Figure 3). Of note, when T cells are activated by anti-CD3 and anti-CD28 in the absence of myeloid cells, we do not observe a statistically significant suppression of T-cell proliferation mediated by mAb 7E12 (Supplementary Figure 3).

In contrast, mAb 8G10 acts as a weak human VISTA antagonist, mildly enhancing the proliferation of both CD4<sup>+</sup> and CD8<sup>+</sup> T cells as compared to ConA activation alone

( $p < .01$ ; Figure 4). Moreover, interferon  $\gamma$  (IFN $\gamma$ ) levels were statistically elevated in human PBMC cultures treated with ConA and 8G10 compared to those treated with ConA alone ( $p < .05$ ; Figure 5).

As shown in Figure 4, Nb7 behaved as a human VISTA agonist based on T-cell proliferation, whereby the proliferation of both CD4<sup>+</sup> and CD8<sup>+</sup> T cells were significantly suppressed when compared to ConA activation alone. However, as shown in Figure 5, levels of IL-2, IFN $\gamma$ , and IL-10 in the human PMBC groups treated with ConA and Nb7 were not statistically different than the levels observed for those treated with ConA alone.

All of the cross-reactive anti-hmVISTA mAbs (3C3, 7C6, 7C7, and 7G1) appear to behave agonistically in the ConA-stimulated human PBMC cultures, reducing the proliferation of CD4<sup>+</sup> and CD8<sup>+</sup> T cells, although to a weaker extent than the mAbs that target human VISTA specifically (Figure 4). None of the anti-hmVISTA mAbs affected the secretion levels of IL-2 and IFN $\gamma$  significantly, but all of them significantly increased the production of the anti-inflammatory cytokine IL-10 (Figure 5).

## Anti-hmVISTA mAb 7G1 reduced the severity of psoriasis-like symptoms in mice

Before testing the cross-species anti-hmVISTA mAbs *in vivo*, the mAbs were first screened in an *ex vivo* experiment on ConA-stimulated mouse splenocytes in a similar set-up as described above for human PBMCs. As shown in Figures 6, 7C6, 7C7, and 7G1 reduced the proliferation of ConA-stimulated CD4<sup>+</sup> T cells significantly (4%, 34%, and 31%, respectively), although the reduction was weak for 7C6. In addition, mouse splenocytes treated with ConA and either 7C7 or 7G1 also displayed lower proliferation rates of CD8<sup>+</sup> T cells as compared to those treated with ConA alone (22% and 20%,

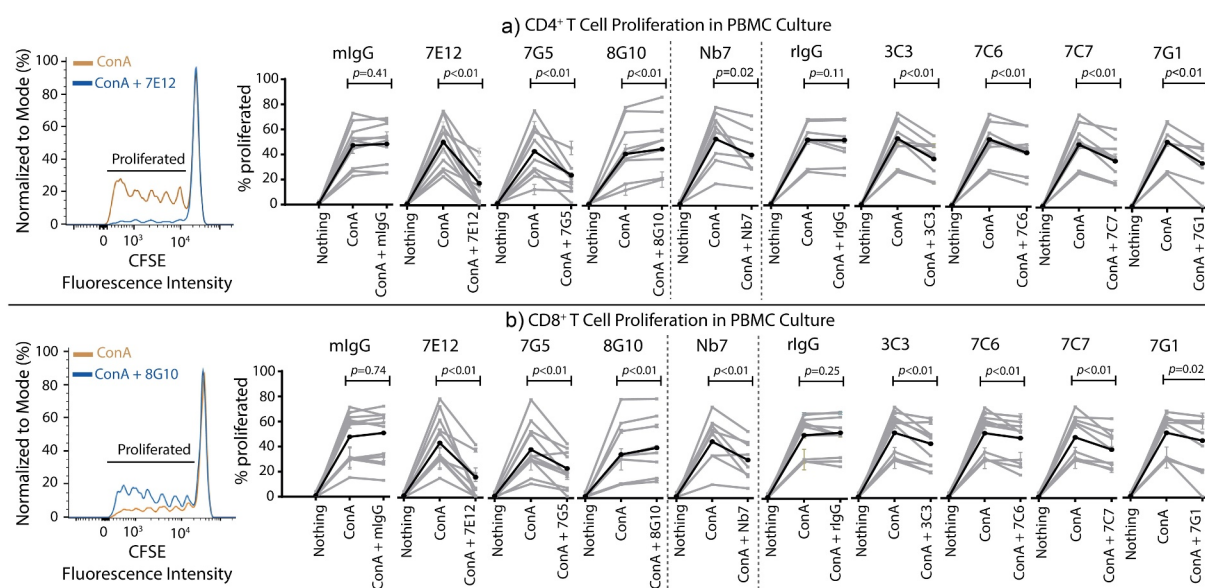


**Figure 4.** Effect of anti-hVISTA mAbs and Nb7 and anti-hmVISTA mAbs on T-cell proliferation in human PBMC cultures. Percentages of proliferated (a) CD4<sup>+</sup> and (b) CD8<sup>+</sup> T cells in human PBMC cultures after stimulation with 1  $\mu\text{g}/\text{mL}$  ConA and anti-hVISTA mouse mAbs (7E12, 7G5, 8G10) and Nb7 or anti-hmVISTA rat mAbs (3C3, 7C6, 7C7, 7G1) for 4 days. Representative CFSE T-cell proliferation profiles are shown on the left side for ConA alone or in the presence of mAb 7E12 (a) or 8G10 (b), normalized to mode (% of counts in the maximum peak). Experiments were performed in replicates on 5 donors. Grey lines represent a separate paired experiment; black lines represent the average of all experiments.

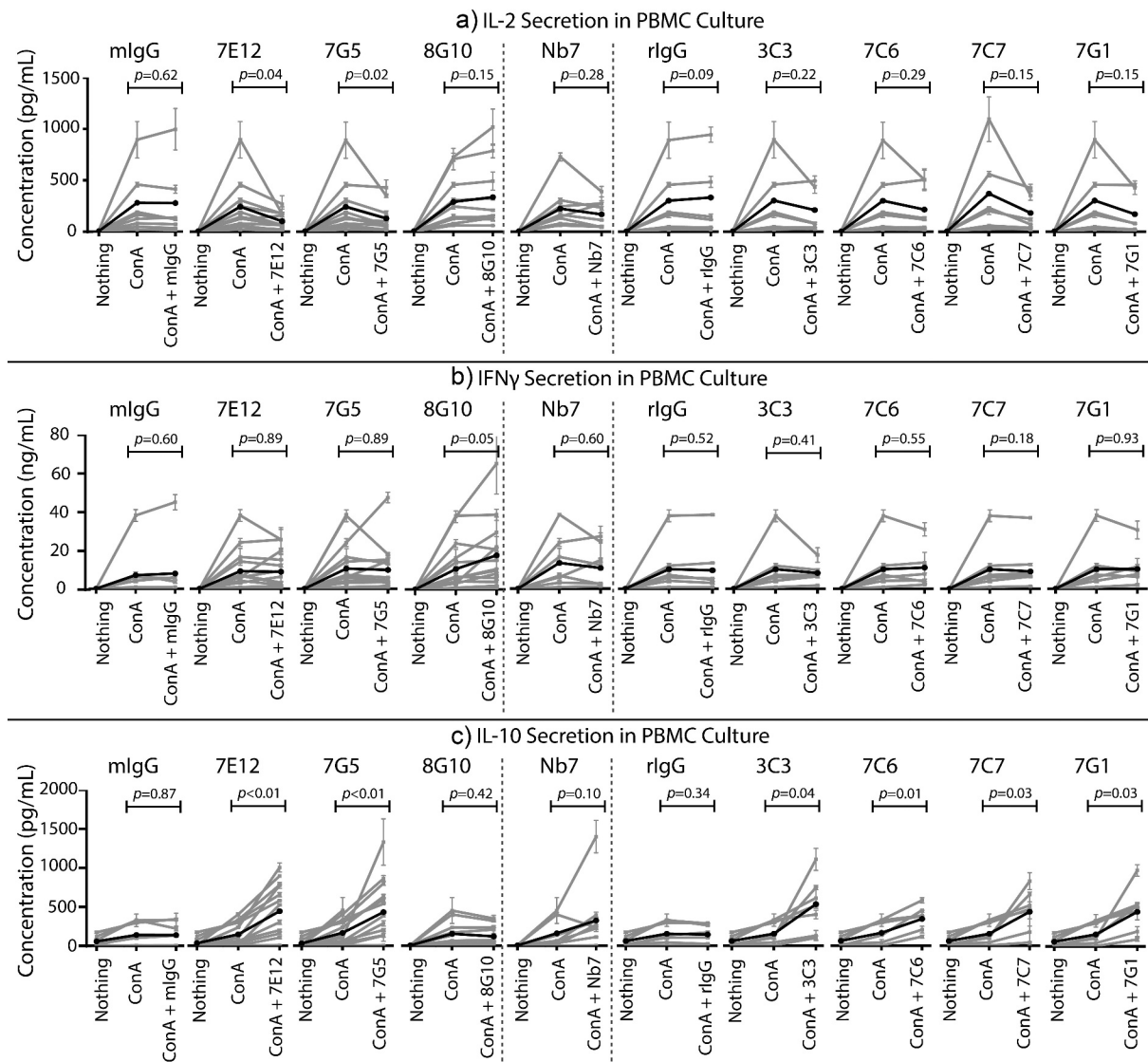


**Figure 5.** Effect of anti-hVISTA mAbs and Nb7 and anti-hmVISTA mAbs on cytokine production in human PBMC cultures. Concentrations of (a) IL-2, (b) IFN $\gamma$ , and (c) IL-10 in human PBMC cultures after stimulation with 1  $\mu$ g/mL ConA and anti-hVISTA murine mAbs (7E12, 7G5, 8G10), anti-hVISTA Nb7, or anti-hmVISTA rat mAbs (3C3, 7C6, 7C7, 7G1) for 2 days. Experiments were performed on 5 donors. Grey lines represent a separate paired experiment; black lines represent the average of all experiments.

respectively), although the differences were not statistically significant. As previously mentioned, the inhibitory mechanism of these mAbs on mouse splenocytes does not appear to be linked to cytotoxicity (Supplementary Figure 3). Therefore, 7C7 and 7G1 were chosen to be further tested *in vivo*.

Agonistic anti-hmVISTA mAbs were tested to treat inflammatory responses in a IMQ-induced psoriasis-like model in mice<sup>15</sup> as VISTA deficiency was previously shown to exacerbate a form of IMQ-induced psoriasis inflammation of the ear.<sup>6</sup> In this model, IMQ cream (62.5 mg) was applied topically on a daily basis to a shaved area of female C57BL/6 mice, where IMQ activates immune responses as a TLR7 and TLR8 ligand. IMQ-treated mice received 100  $\mu$ g of an mAb intraperitoneally every other day. As Figure 7a shows, 7G1 significantly reduced the severity score of IMQ-induced psoriasis-like skin inflammation. Interestingly, although 7C7 also ameliorated the symptoms of skin inflammation, the degree of change was less than that of rat

IgG2a control. Since IL-17 and TH17 cells play a pivotal role in psoriasis, IL-17 expression level in the skin was measured by qPCR. As demonstrated in Figure 7b, IL-17 expression was significantly increased after IMQ stimulation, and was significantly reduced by both 7C7 and 7G1 (by 50% and 53%, respectively), and not by rat IgG2a control. Meanwhile, the expression of pro-inflammatory cytokine IFN $\gamma$  was significantly lowered by 7G1 (by 36%) only (Figure 7c). Finally, since the depletion of T cells had been shown to attenuate psoriasis-like symptoms,<sup>15</sup> the effect of mAbs on T-cell populations in the spleen was measured using flow cytometry. Indeed, mice treated with 7G1 displayed a significant reduction in the percentage of CD4<sup>+</sup> T cells in the spleen (Figure 7d), although the change in CD8<sup>+</sup> T cells was not significant. Overall, 7G1 is a strong agonist of human and murine VISTA that not only reduces the proliferation of T cells and pro-inflammatory cytokine secretion *ex vivo*, but also attenuates psoriasis-like inflammation *in vivo*.

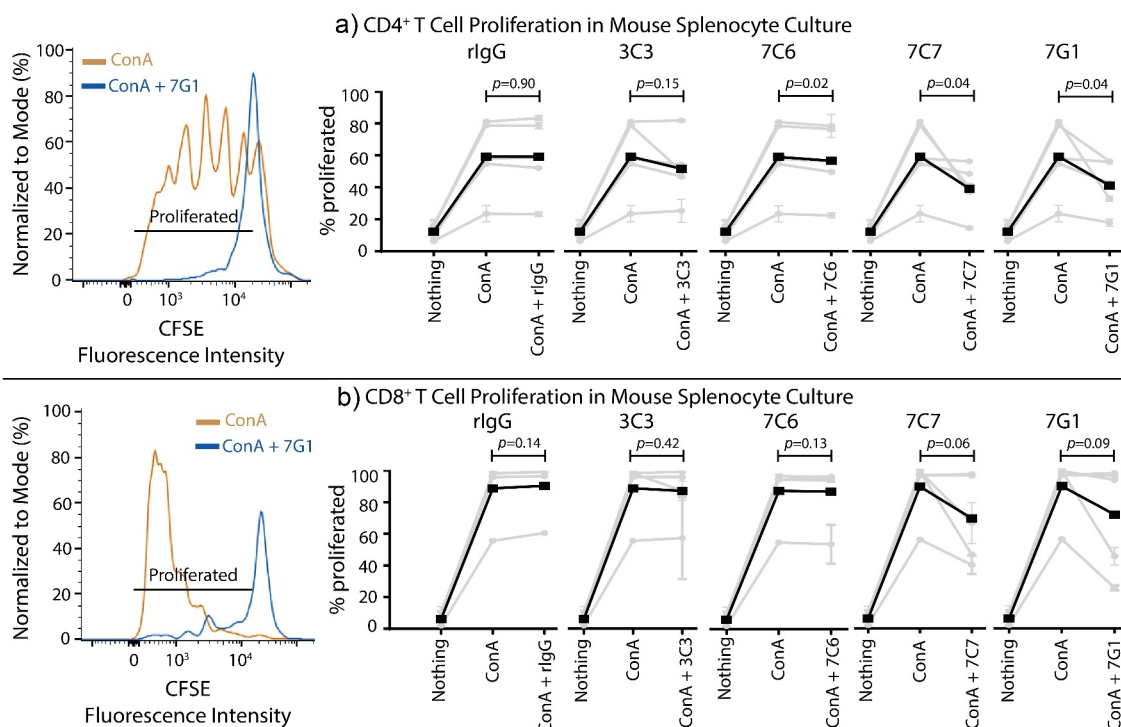


**Figure 6.** Effect of anti-hmVISTA rat mAbs on T-cell proliferation in mouse splenocyte cultures. Percentages of proliferated (a) CD4<sup>+</sup> and (b) CD8<sup>+</sup> T cells in mouse splenocyte cultures after stimulation with 1  $\mu$ g/mL ConA and anti-hmVISTA rat mAbs for 3 days. Representative CFSE T-cell proliferation profiles are shown on the left side for ConA alone or in the presence of mAb 7G1, normalized to mode (% of counts in the maximum peak). Each gray line represents a biological replicate (separate paired experiment performed on a different mice); black lines represent the average of all experiments.

## Discussion

VISTA is part of a co-inhibitory immune pathway where it functions as both a ligand and a receptor. Since the VISTA pathway is functionally distinct from the PD-1:PD-L1 axis, it suggests that VISTA antagonists may be paired with approved immune checkpoint inhibitors in cancer immunotherapy. As important, VISTA agonists may be valuable in treating inflammation and auto-immunity. Herein, we describe the generation and functional characterization of murine mAbs and heavy chain single domain antibody fragments (Nbs) that specifically bind to the human VISTA extracellular domain, as well as rat mAbs that bind to both human and murine VISTA. Importantly, the study identified two strongly agonistic anti-hVISTA mAbs (7E12 and 7G5) that suppress T-cell proliferation in ConA-stimulated human PBMC cultures; and an agonistic anti-hmVISTA mAb (7G1) that attenuated IMQ-induced psoriasis *in vivo*.

All VISTA binders bound with nanomolar (nM) affinities to human or human/murine VISTA (Figure 2). In contrast, studies have shown that monomeric forms of IgV domains, PD1/PD-L1, for example, interact with each other in the low micromolar ( $\mu$ M) range.<sup>16</sup> These anti-VISTA mAbs and Nbs detected VISTA in the context of both ELISA and flow cytometry experiments. Interestingly, Nb7 displayed the fastest dissociation constant upon binding to hVISTA, yet generated the strongest mean fluorescence intensity signal of all 3 Nbs in detecting VISTA-expressing CD14<sup>+</sup>CD16<sup>-</sup> human monocytes and hVISTA transiently expressed on Expi293F cells by flow cytometry (Figure 3).

Since a previously reported agonistic mAb against murine VISTA was able to protect mice from ConA-induced hepatitis,<sup>8</sup> we tested our anti-human VISTA biologics for their therapeutic potential by studying their effect on a ConA-stimulated human PBMC culture. ConA is a lectin that has been shown to pan-activate immune cells including T cells and further induce T cell-mediated tissue inflammation in mice.<sup>17</sup> Here, mAb 8G10 increased the proliferation of CD4<sup>+</sup> and CD8<sup>+</sup> T cells slightly (Figure 4) and enhanced the production of IFN $\gamma$  in ConA-stimulated human PBMC cultures. This result suggests that 8G10 may act as a hVISTA antagonist, which may reflect its ability to block the interaction between human VISTA on monocytes and VISTA receptors on T cells. In contrast, all other mAbs and Nb7 reduced the proliferation of human T cells (Figure 4). However, based on minimal changes in expression patterns observed for both pro- and anti-inflammatory cytokines relative to the ConA activation of whole human PBMCs from multiple donors, Nb7 does not represent a strong human VISTA agonist (Figure 5).

Treatment of ConA-activated human PBMCs with anti-hVISTA mAbs 7E12 and 7G5 strongly inhibited CD4<sup>+</sup> and CD8<sup>+</sup> T-cell proliferation and reduced the production of IL-2, a T cell-activating cytokine,<sup>18</sup> while increasing the expression of IL-10, which inhibits T-cell proliferation and IL-2 production,<sup>19</sup> confirming them as human VISTA agonists (Figures 4 and 5). The binding characteristics of each of the human-specific mAbs are very similar, with  $k_{on}$ ,  $k_{off}$ , and  $K_D$  values within a close range, including the functionally distinct mAb 8G10. Regarding the mildly antagonistic function of mAb 8G10, neither the affinity nor the competition analysis

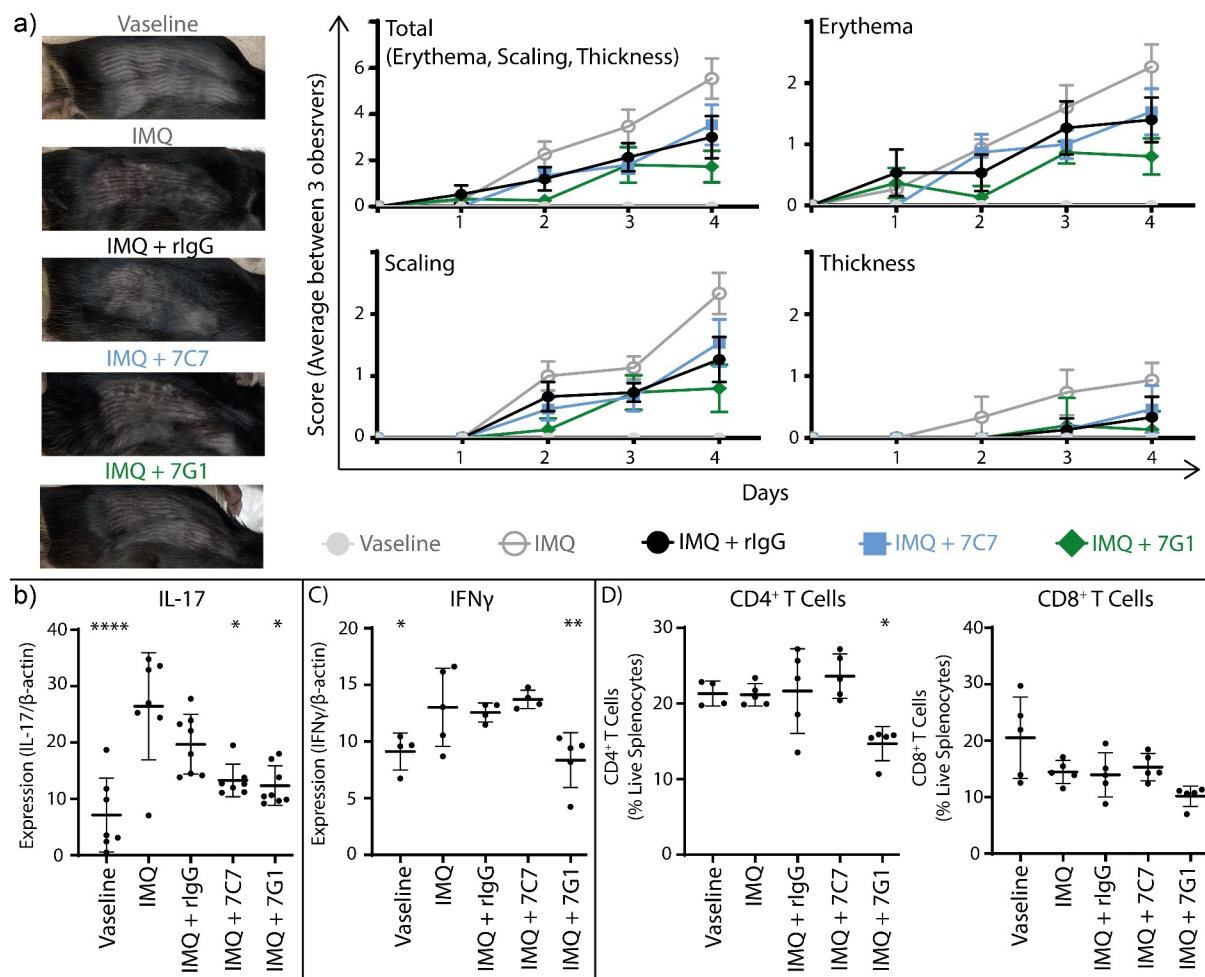


**Figure 7.** Effect of rat anti-hmVISTA mAbs on the inflammatory and immune status of mice treated topically with Imiquimod (IMQ). IMQ cream or Vaseline was topically applied daily to shaved areas on the back of female C57BL/6 mice. IMQ-treated mice received intraperitoneal injections of rat anti-hmVISTA mAbs, rIgG, or PBS every other day. (a) Graph showing the cumulative score representing the severity of psoriasis-like skin inflammation (erythema, scaling, and thickness, each out of 4; average of 3 independent scorers), with adjusted *p*-values comparing each group (*n* = 5 from 1 trial) to IMQ alone. (b) RNA expression of IL-17 in treated skin samples of mice sacrificed on day 3 (*n* = 8 from 2 trials). (c) RNA expression of IFN $\gamma$  in skin samples recovered from mice sacrificed on day 6 (*n* = 5 from 1 trial). (d) Percentage of CD4<sup>+</sup> and CD8<sup>+</sup> T cells in splenocytes harvested from mice sacrificed on day 6, as determined by flow cytometry (*n* = 5 from 1 trial). Data is shown as mean  $\pm$  SD, each dot represents a mouse in the experimental group. \**p* < .05, \*\**p* < .01, \*\*\**p* < .001, \*\*\*\**p* < .0001 relative to IMQ+rIgG groups by Student's *t*-test adjusted for multiple comparisons.

appears to account for this difference. One cannot discern from SPR analyses if a competing antibody is binding to a nearby or overlapping epitope that may be blocked by the primary binder (sterical hindrance). The cross-reactive mAbs have a lower affinity toward hVISTA, and may account for their reduced potency. Importantly, VISTA is constitutively expressed on both myeloid and lymphoid cells.<sup>4,20</sup> This finding, combined with the observed lack of suppression of T-cell proliferation by these mAbs in the absence of myeloid cells (Supplementary Figure 3B), suggests that the agonistic potential of these mAbs may be mediated both through the direct suppression of T cells and indirectly via the high expression of VISTA in the myeloid compartment, where suppressed monocytes downregulate T-cell activation. This 2-prong mechanistic model is further supported by a recent study that defined the effect of VISTA agonism on cells of the myeloid lineage.<sup>21</sup> Future research will be aimed at delineating the effects each of the mAbs play on specific subsets of T cells and myeloid cells.

Similarly, the agonistic property of anti-hmVISTA mAbs were tested using mouse splenocytes and in an *in vivo* mouse model of IMQ-induced psoriasis. All of the anti-hmVISTA mAbs detected VISTA expression on murine macrophages, neutrophils, and CD4<sup>+</sup> cells, with 7G1 being the strongest binder to these VISTA-expressing immune cell populations (Figure 3b). However, only 7C7 and 7G1 reduced the proliferation of CD4<sup>+</sup> T cells in ConA-stimulated mouse splenocyte cultures (Figure 6); and only 7G1 was able to alleviate the severity of IMQ-induced psoriasis-like skin inflammation beyond rat IgG control (Figure 7a). The most surprising result in this model was the ability of the rat IgG2a control to attenuate IMQ-induced inflammation. This finding may be due to the mild cytotoxicity of the rIgG2a control used (Supplementary Figure 3C) or the sialylation of this IgG as shown by the anti-inflammatory properties of purified IgG fractions given intravenously during gamma globulin therapy.<sup>22</sup> Further investigation would be necessary to explain the anti-inflammatory effect observed in our model. The potential of



mAb 7G1 to reduce the severity of psoriasis-like symptoms may be linked to its ability to reduce splenic T cells to comparative levels expected for a healthy mouse (~25% CD3<sup>+</sup> T cells) compared to IMQ-treated mice (Figure 7d) and the epidermal expression of IL-17 (Figure 7b), a critical cytokine in the development of plaque-like psoriasis.<sup>15</sup> Of note, the control group of mice receiving Vaseline only had an abnormally high percentage of T cells in the spleen which may be the result of systemic effects likely caused by ingestion of the Vaseline. Furthermore, IFN $\gamma$  gene expression is reduced by mAb 7G1 (Figure 7c). IFN $\gamma$  represents a prognostic marker of psoriasis where a decrease in IFN $\gamma$  predicts a lower score in terms of psoriasis severity,<sup>23</sup> although data on the level of IFN $\gamma$  observed between psoriatic lesions and healthy controls remain contradictory.<sup>24</sup> This observation may explain why no difference was found between IFN $\gamma$  levels in Vaseline- and IMQ-treated mice. Additionally, two groups have now reported the importance on type I IFNs in the development of psoriatic lesions.<sup>25,26</sup> A recent study led by ElTanbouly reported that VISTA agonism almost completely suppresses the type I IFN pathway.<sup>21</sup> Future assessment of the effect of the mAbs generated herein, in particular 7G1, on the type I IFN pathway is necessary to fully elucidate their mechanism of action in this context.

In this study, we did not identify anti-VISTA Nbs as useful agonists or antagonists, suggesting that the bio-panning strategy used in generating these anti-VISTA Nbs needs to be re-assessed. Alternative selection criteria, stringency in the method, or alternative immunization strategies may yield more favorable binders, potentially with antagonistic and/or cross-reactive properties. Furthermore, alternative Nb engineering strategies, bivalency, for example, may improve upon the therapeutic potential of all Nbs described in this study.

Likewise, the lack of strong mAb antagonists is surprising. We cannot exclude the possibility that when agonizing VISTA on monocytes or T cells, in this context, we are not simultaneously antagonizing the cognate VISTA receptor. Further studies are needed in the context of alternative microenvironments. For instance, it is difficult to ascertain the functionality of these biologics in a tumor microenvironment where the predominant source of VISTA are cells that are phenotypically suppressive, such as MDSCs<sup>27,28</sup> and tumor-associated macrophages.<sup>29,30</sup> As these cells are already immune-suppressive, engaging VISTA on these types of cells may not favor further suppressive signaling, but rather block VISTA from binding its cognate receptor, releasing VISTA-mediated T-cell suppression within the tumor microenvironment.

In conclusion, we have generated a panel of mAbs and Nbs targeting human VISTA and demonstrated their utility in detecting the presence of human VISTA in ELISA and flow cytometry assays. Importantly, we demonstrated the agonistic properties of anti-hVISTA mAbs 7E12 and 7G5 on human PBMCs in the context of an inflammation-driven microenvironment (ConA stimulation) and the ability of agonist anti-hVISTA mAb 7G1 in attenuating IMQ-induced psoriasis-like skin inflammation. These findings suggest that these agonistic anti-VISTA mAbs may prove useful in treating inflammatory or auto-immune diseases.

## Materials and methods

### Monoclonal antibody production

Hybridomas producing mAbs against recombinant human or murine VISTA (hVISTA or mVISTA) were generated by ImmunoPrecise Antibodies (Victoria, BC, Canada) by using a pentameric form comprising the extracellular IgV domain of human or murine VISTA (hVISTA-COMP or mVISTA-COMP)<sup>31</sup> as the immunogen for vaccinating Balb/c mice or Lewis rats, respectively. Hybridomas were maintained in Dulbecco's modified Eagle medium (DMEM) (319-016-CL; WISENT) supplemented with 20% HyClone FetalClone II Serum (SH3010903; Cytiva), 1% penicillin-streptomycin (P/S) (450-200-EL; WISENT), 1X HT Supplement (11067030; Gibco), 1X 2-mercaptoethanol (M6250; MilliporeSigma), and 25 mM HEPES (15630056; Gibco). Hybridomas were adapted to growth in H-CELL serum-free medium (001-035-CL; WISENT) for mAb purification. mAbs were purified from culture supernatants using HiTrap protein G HP columns (17040401; Cytiva) and eluted with 0.1 M glycine-HCl (pH 2.7) neutralized with 1 M Tris-HCl (pH 9.0). The recovered mAb preparations were buffer-exchanged into phosphate-buffered saline (PBS) using PD-10 columns (17085101; Cytiva), detoxified by passage through endotoxin removal columns (88274; Thermo Fisher Scientific) then either used immediately or stored at -20°C. The purity of mAbs was assessed by SDS-PAGE and Western blot using anti-mouse and anti-rat IgG heavy and light chain Ab conjugated to horseradish peroxidase (HRP) (A110-105P; Bethyl Laboratories).

### Monoclonal antibody sequencing

mAbs were sequenced by RT-PCR followed by Sanger sequencing. Briefly, RNA was isolated from hybridomas using TRIzol Reagent (15596026; Thermo Fisher Scientific) and cDNA was synthesized using the SensiFAST cDNA synthesis kit (BIO-65053; Meridian Bioscience). Touch-down PCR was performed using DreamTaq DNA Polymerases (EP0701; Thermo Fisher Scientific) on a set of degenerate primers designed to sequence mouse<sup>32</sup> and rat<sup>33</sup> immunoglobulins (Integrated DNA Technologies). PCR amplification products were checked using agarose gel electrophoresis. PCR reactions that produced single products were treated with ExoSAP-IT PCR product cleanup reagent (78200.200.UL; Thermo Fisher Scientific) and sent in for Sanger sequencing at the Center for Applied Genomics (Hospital for Sick Children, Toronto, ON, Canada). Sequences were aligned against the IMGT database<sup>34</sup> using IgBlast ([www.ncbi.nlm.nih.gov/igblast/](http://www.ncbi.nlm.nih.gov/igblast/); National Center for Biotechnology Information, Bethesda, MD, USA)<sup>35</sup> and grouped based on heavy chain CDR3 similarity using Clustal Omega ([www.ebi.ac.uk/Tools/msa/clustalo/](http://www.ebi.ac.uk/Tools/msa/clustalo/); EMBL-EBI, Hinxton, Cambridgeshire, UK).<sup>36</sup>

### Immunization, library construction, and screening for nanobodies

Nanobodies (Nbs) were generated as previously described.<sup>37</sup> Briefly, a llama (*Lama glama*) was immunized once weekly for 6 consecutive weeks with a preparation of hVISTA-COMP

mixed with Gerbu LQ 3000 adjuvant (Gerbu Biotechnik GmbH). A Nb phage library was constructed following total RNA extraction and cDNA subcloning into the phagemid vector pMECS. *Escherichia coli* TG1 cells were transformed with this vector yielding  $2 \times 10^8$  transformants with 100% insert. Following four rounds of phage display panning using hVISTA-COMP, crude periplasmic extracts from 191 individual colonies were screened by ELISA for specificity toward hVISTA. Positive clones were selected for DNA sequencing (VIB sequencing facility, Flanders, Belgium). Sequence analysis was performed using CLC Main Workbench 8 software (Qiagen) and manually annotated in accordance to the IMGT numbering system.<sup>34</sup> Selected anti-hVISTA Nbs were transformed into *Escherichia coli* WK6 to facilitate production.

### Nanobody production

The expression and purification of Nbs followed protocols previously described.<sup>38</sup> Briefly, 1 mL of an overnight starter culture of each of the clones was inoculated into 330 mL of Terrific Broth (TB) medium supplemented with 100 µg/ml ampicillin and 0.1% glucose and grown at 37°C in shaking flasks (200 RPM) until OD<sub>600nm</sub> reached 0.6–0.8. The cultures were subsequently induced by adding 1 mM isopropyl-β-D-thiogalactopyranoside (IPTG) and further incubated at 28°C overnight (200 RPM). Cells were later harvested by centrifugation and incubated in 4 mL of TES (0.5 mM EDTA, 0.2 M Tris-HCL, 0.5 M sucrose, pH8.0) on ice, shaking (200 RPM) for 6 hours. An 8 mL aliquot of 0.25× TES (diluted in water) was then added to each cell suspension and the resulting mixtures incubated for an additional 12–15 hours before periplasmic extracts were collected via centrifugation. Nbs were purified from these extracts using immobilized metal affinity chromatography (IMAC) on a His-Trap column (17524802; Cytiva) and eluted with 0.5 M Imidazole (1047160250; MilliporeSigma) in PBS. The eluted Nb fractions were desalted using PD-10 desalting columns (17085101; Cytiva) and detoxified using high-capacity endotoxin removal columns (88274; Thermo Fisher Scientific). The Nbs were either used immediately or stored at –20°C. The purity of each Nb was assessed by SDS-PAGE and Coomassie Blue staining. Western blot using a biotinylated anti-HA antibody (12158167001; MilliporeSigma) and streptavidin-HRP (RABHRP3; MilliporeSigma) was performed to confirm the presence of a Nb. A Nb (Nb19) targeting the babA adhesion molecule of *H. pylori*,<sup>39</sup> was used as a negative control.

### Surface plasmon resonance

Binding kinetics of mAbs and Nbs to hVISTA and mVISTA were obtained by SPR using a BIAcore T200 (Cytiva) and HBS running buffer (20 mM of HEPES pH 7.4, 150 mM NaCl, 0.005% Tween-20, 3.4 mM EDTA). Briefly, anti-histidine antibodies were immobilized on a CM5 chip (29149604; Cytiva) using the His capture kit (28995056; Cytiva) following manufacturer's protocol. For mAbs, VISTA was captured by flowing 30 µg/mL of hVISTA-COMP-his or mVISTA-COMP-his at a flow rate of 30 µL/min. Sensorgrams were collected using single-cycle kinetics covering five mAb concentrations (1:2

serial dilutions). For Nbs, solutions of each nanobody (30 µg/mL) were flown over an anti-histidine-coated chip. Five concentrations (1:2 serial dilutions) of hVISTA-Fc (produced in house) were then injected at a flow rate of 30 µL/min.  $K_D$ ,  $k_{on}$ , and  $k_{off}$  were calculated by analyzing the sensorgrams with a 1:1 Langmuir binding model after subtracting reference sensorgrams.

For epitope binning analysis, hVISTA-Fc was immobilized on a CM5 chip (29149604; Cytiva) via amine coupling (pH 4.5). mAb “A” was injected at a flow rate of 30 µL/min for 600 s at a concentration 200× its  $K_D$  value. Subsequently, a mixture of mAbs “A” and “B”, both at concentration 200× their respective  $K_D$  values, was injected under the same conditions, and the response unit (RU) was monitored for an additional 600 s followed by regeneration. Due to the large size difference between mAbs and Nbs, an alternative approach was taken to assess epitope binning of a representative mAb/Nb pair. In this instance, Nb1 was immobilized, to a point of saturation, on an anti-histidine-coated chip. hVISTA-Fc was subsequently injected at a saturating concentration. Finally, mAb 7E12 was injected at a concentration 200× the  $K_D$  value. The RU was monitored for an additional 600 s followed by regeneration.

### Competition ELISA

To confirm the specificity of the Nbs to hVISTA, a competition ELISA was performed against anti-hVISTA mAbs. ELISA plate wells (44–2404-21; Thermo Fisher Scientific) were coated with hVISTA-COMP (10 µg/ml) and subsequently blocked with 0.5% milk. Nbs (330 nM) were then dispensed into wells alone or in combination with 2-fold molar excess of mAbs, mouse IgG1 control (400165; BioLegend), or rat IgG2a control (400543; BioLegend), and incubated for 1 h at room temperature. hVISTA:Nb complexes were detected using a biotinylated anti-HA antibody (12158167001; MilliporeSigma), followed by streptavidin HRP (RABHRP3; MilliporeSigma) and the substrate TMB (3,3',5,5'-tetramethylbenzidine) (34028; Thermo Fisher Scientific). Absorbance readings were recorded at 450 nm.

### Mice

Female C57BL/6 mice at 8–10 weeks of age (The Jackson Laboratory) were used throughout this study and housed at the Sunnybrook Research Institute (SRI; Sunnybrook Health Sciences Center, Toronto, ON, Canada) Comparative Research (SRICR) facility. All protocols were approved by the SRICR Animal Care Committee, accredited by the Canadian Council of Animal Care.

### Direct cell binding assay

Binding of mAbs and Nbs to human and murine immune cells were tested using human PBMCs and mouse splenocytes. For binding on human cells, whole human blood was obtained from donors in accordance with guidelines set forth by the Sunnybrook Research Ethics board (REB approval number 443–2017). Human PMBCs were isolated from whole blood using Ficoll Paque PLUS (1.077 g/ml) (17144003; Cytiva).

PBMCs had their Fc receptors blocked with Human TruStain FcX (422301; BioLegend) then incubated with 2.5 µg of mAb, mouse IgG1 (401408; BioLegend), or rat IgG2a (400565; BioLegend) or 15 µg Nb for 1 h at 4°C. After washing with PBS, the PBMCs were incubated with secondary antibodies (1 µL; FITC anti-mouse IgG1, FITC anti-HA, or FITC anti-rat IgG2a; 406605, 901507, or MRG2a-83; BioLegend) or control FITC anti-VISTA antibodies (clone B7H5DS8; 11-1088-42; eBioscience) for 40 minutes at 4°C. A staining cocktail consisting of PE/Cy5 anti-CD11b (101210; BioLegend), APC/Cy7 anti-CD14 (325620; BioLegend), Alexa Flour 700 anti-CD16 (302026; BioLegend), PE/Cy7 anti-CD4 (317414; BioLegend), and Alexa Flour 647 anti-CD8 (301022; BioLegend) was then added to the PBMCs and incubated for 20 minutes at 4°C. Finally, the PBMCs were washed and resuspended in 3 µM DAPI (D1306; Thermo Fisher Scientific) and cytometric profiles recorded using a BD LSR II flow cytometer (BD) maintained by The Center for Flow Cytometry & Scanning Microscopy (CCSM) at Sunnybrook Research Institute (SRI; Sunnybrook Health Sciences Center, Toronto, ON, Canada). The same protocol was performed on murine splenocytes to measure the binding of rat anti-hmVISTA mAbs to murine immune cells. The staining cocktail consisted of APC/Cy7 anti-CD45 (147718; BioLegend), BV510 anti-CD11b (101263; BioLegend), Alexa Flour 700 anti-CD3 (100216; BioLegend), Alexa Flour 647 anti-CD8 (100724; BioLegend), PE/Dazzle 594 anti-Ly6C (128044; BioLegend), PE/Cy7 anti-Ly6G (127618; BioLegend), FITC anti-F4/80 (123108; BioLegend), Pacific Blue anti-MHCII (107620; BioLegend), and PerCP/Cy5.5 anti-CD11c (117328; BioLegend).

Additionally, Expi293F cells were transiently transfected with pcDNA 3.4 TOPO vector containing the gene for hVISTA (Q9H7M9) (ThermoFisher Gene Art Gene Synthesis). Cells were harvested 72 hours post-transfection, washed with PBS, and incubated with 2.5 µg of mAbs, mouse IgG1 (401408; BioLegend), rat IgG2a (400565; BioLegend), or 15 µg Nb for 1 hour at 4°C. After washing with PBS, the cells were incubated with secondary antibodies (1 µL; FITC anti-mouse IgG1, FITC anti-HA, or FITC anti-rat IgG2a; 406605, 901507, or MRG2a-83; BioLegend) or a control FITC-labeled anti-VISTA antibody (clone B7H5DS8; 11-1088-42; eBioscience) for 40 minutes at 4°C. Finally, cells were washed and resuspended in 3 µM DAPI (D1306; Thermo Fisher Scientific) followed by fluorescence-activated cell sorting analysis as described above.

### ***T-cell proliferation and cytokine assays on human PBMCs***

Human PBMCs were stained with 5 µM CFSE (C34554; Thermo Fisher Scientific) and cultured in X-VIVO 15 medium (BE02-060 F; Lonza) supplemented with 5% fetal bovine serum (FBS; 080-450; WISENT) in round-bottom 96-well plates at 30,000 cells per well. ConA (1 µg/mL; C5275; MilliporeSigma) was used to stimulate the PBMCs and 15 µg/mL of either mAbs, mouse IgG1 controls (400165; BioLegend), rat IgG2a controls (400544; BioLegend), or Nbs were added and topped up to 300 µL per well. Supernatants were collected on day 2 for cytokine analyses using LegendPlex kits for IL-2, IFN $\gamma$ , and IL-

10 (BioLegend). One representative cross-reactive mAb (3C3) was titrated using 15, 10, 5, or 1 µg/mL, from which 15 µg/mL was determined to be the best working concentration.

Alternatively, CD3<sup>+</sup> T cells were purified from the PBMC population using the EasySep Human T Cell Isolation Kit (17951; Stem cell Technologies). The T cells were stained with 5 µM CFSE (C34554; Thermo Fisher Scientific) and cultured in X-VIVO 15 medium (BE02-060 F; Lonza) supplemented with 5% FBS in round-bottom 96-well flat bottom plates at 20,000 cells per well. T cells were stimulated with ImmunoCult (10971; StemCell Technologies) and 15 µg/mL of 7E12 or mouse IgG1 control (400165; BioLegend) was added and the final volume adjusted to 200 µL per well. Cells were collected after 4 days of culture, stained as described above, and analyzed by flow cytometry to measure T-cell proliferation.

### ***Cytotoxicity assay***

Cytotoxicity assays were performed as previously described.<sup>40</sup> In brief, 10<sup>5</sup> human PBMCs or total murine splenocytes were cultured in 100 µL of X-VIVO 15 medium (BE02-060 F; Lonza) supplemented with 5% FBS in the presence or absence of 15 µg/mL of either mAbs, mouse IgG1 controls (400165; BioLegend), or rat IgG2a controls (400544; BioLegend). Following 4-h incubation at 37°C, supernatants were collected and assayed via a lactate dehydrogenase kit in accordance to the manufacturer instructions (ab65393; Abcam). Percent cytotoxicity was calculated with the following formula: cytotoxicity (%) = ((Test Sample – Low Control)/(High Control – Low Control)) × 100.

### ***Mouse splenocyte proliferation assay***

Mouse splenocytes were treated with red blood cell lysis buffer, stained with 5 µM CFSE (C34554; Thermo Fisher Scientific), and cultured in X-VIVO 15 medium (BE02-060 F; Lonza) supplemented with 5% FBS (080-450; WISENT) in round-bottom 96-well plates at 30,000 cells per well. ConA (2 µg/mL; C5275; MilliporeSigma) was used to stimulate the PBMCs and 15 µg/mL of each mAb or a rat IgG2a control (400544; BioLegend) were added and topped up to 300 µL per well. Cells were collected after 4 days of culture, stained with a cocktail consisting of APC/Cy7 anti-CD45 (147718; BioLegend), Alexa Flour 700 anti-CD3 (100216; BioLegend), Alexa Flour 647 anti-CD8 (100724; BioLegend), and PE/Cy7 anti-CD4 (100422; BioLegend), and analyzed by flow cytometry.

### ***IMQ-induced psoriasis in mice***

Ten-week old female C57BL/6 mice were treated with a daily dose of 62.5 mg of imiquimod (IMQ) cream (Zyclra; 3.75% w/v) or petroleum jelly (Vaseline) control applied evenly on their shaven back with a cotton swab. Daily doses (100 µg) of either an anti-hmVISTA mAb, or a rat IgG2a control (400544; BioLegend), or PBS were injected intraperitoneally into control or IMQ-treated mice. Mice were monitored daily for severity of the psoriasis-like skin conditions: erythema, scaling, and

**Table 1.** Gene-specific primers used in qPCR.

Target Gene	Forward Primer	Reverse Primer
$\beta$ -actin	GTGGGCCGCTCTAGACACCA	CGTTGGCCTTAGGGTTCAGGGGGC
IL-17	AAGGCAGCAGCGATCATCC	GGAACGGTTGAGGTAGTCTGAG
IFN $\gamma$	TGAGTATTGCCAAGTTTGAGGTCA	CGCAACAGCTGGTGGAC

thickness.<sup>15</sup> Each of the conditions were scored from 0 to 4, with four being very marked, by three independent scorers who were blinded to the treatment type.

Mice were sacrificed on days 3 and 6 and had their skin harvested for qPCR analysis to profile for gene expression. Briefly, skin areas that were shaven and treated with IMQ or Vaseline cream were excised and chopped finely before being treated with TRIzol Reagent (15596026; Thermo Fisher Scientific) to isolate RNA contents, which were then reverse-transcribed using high-capacity cDNA reverse transcription kit (4368814; Thermo Fisher Scientific). qPCR was performed with the SensiFAST SYBR no-ROX kit (BIO-98005; Meridian Bioscience) and gene-specific primers listed in Table 1 (Integrated DNA Technologies) and read on the Mastercycler ep realplex qPCR instrument (Eppendorf). In addition, mice sacrificed on day 6 had their splenocytes harvested and profiled for CD4<sup>+</sup> and CD8<sup>+</sup> T cells with a staining cocktail containing APC/Cy7 anti-CD45 (147718; BioLegend), Alexa Flour 700 anti-CD3 (100216; BioLegend), Alexa Flour 647 anti-CD8 (100724; BioLegend), and PE/Cy7 anti-CD4 (100422; BioLegend).

## Statistics

Each PBMC experiment was repeated on 5 different donors that were randomized between groups. Student's t-test (2-tail, paired, adjusted for multiple comparisons where necessary) was applied to test significance between PBMCs treated with ConA alone or ConA in the presence of mAbs or Nbs (significance was taken at  $\alpha = 0.05$ ).

## Acknowledgments

This work was supported by CIHR Project grants PJT148556 and PJT156138 to JG. Furthermore, the authors would like to acknowledge the nurses at the Sunnybrook transfusion medicine clinic and the blood donors for their contribution.

## Disclosure statement

No potential conflict of interest was reported by the author(s).

## Funding

This work was supported by the Canadian Institutes of Health Research [PJT148556, PJT156138].

## References

- Pardoll DM. The blockade of immune checkpoints in cancer immunotherapy. *Nat Rev Cancer*. 2012;12:252–13.
- Flies DB, Wang S, Xu H, Cutting Edge: CL, Monoclonal Antibody A. Specific for the programmed death-1 homolog prevents graft-versus-host disease in mouse models. *J Immunol*. 2011;187:1537–41.
- Wang L, Rubinstein R, Lines JL, Wasiuk A, Ahonen C, Guo Y, Lu L-F-F, Gondek D, Wang Y, Fava RA, et al. Vista, a novel mouse Ig superfamily ligand that negatively regulates T cell responses. *J Exp Med*. 2011;208:577–92.
- Lines JL, Pantazi E, Mak J, Sempere LF, Wang L, O'Connell S, Ceeraz S, Suriawinata AA, Yan S, Ernstoff MS, et al. Vista is an immune checkpoint molecule for human T cells. *Cancer Res*. 2014;74:1924–32.
- Le Mercier I, Chen W, Lines JL, Day M, Li J, Sergent P, Noelle RJ, Wang L. Vista regulates the development of protective antitumor immunity. *Cancer Res*. 2014;74:1933–44.
- Li N, Xu W, Yuan Y, Ayithan N, Imai Y, Wu X, Miller H, Olson M, Feng Y, Huang YH, et al. Immune-checkpoint protein Vista critically regulates the IL-23/IL-17 inflammatory axis. *Sci Rep*. 2017;7:1485.
- Flies DB, Higuchi T, Chen L. Mechanistic assessment of PD-1H coinhibitory receptor-induced T cell tolerance to allogeneic antigens. *J Immunol*. 2015;194:5294–304.
- Flies DB, Han X, Higuchi T, Zheng L, Sun J, Ye JJ, Chen L. Coinhibitory receptor PD-1H preferentially suppresses CD4<sup>+</sup> T cell-mediated immunity. *J Clin Invest*. 2014;124:1966–75.
- ElTanbouly MA, Zhao Y, Nowak E, Li J, Schaafsma E, Le Mercier I, Ceeraz S, Lines JL, Peng C, Carriere C, et al. Vista is a checkpoint regulator for naïve T cell quiescence and peripheral tolerance. *Science* (80-). 2020;367:eaay0524.
- Yoon KW, Byun S, Kwon E, Hwang S-YS-Y, Chu K, Hiraki M, Jo S-HS-H, Weins A, Hakrrouch S, Cebulla A, et al. Control of signaling-mediated clearance of apoptotic cells by the tumor suppressor p53. *Science* (80-). 2015;349:1–34.
- Ceeraz S, Sergent PA, Plummer SF, Schned AR, Pechenick D, Burns CM, Noelle RJ. Vista deficiency accelerates the development of fatal murine lupus nephritis. *Arthritis Rheumatol*. 2017;69:814–25.
- Liu H, Li X, Hu L, Zhu M, He B, Luo L, Chen L. A crucial role of the PD-1H coinhibitory receptor in suppressing experimental asthma. *Cell Mol Immunol*. 2018;15:838–45.
- Han X, Vesely MD, Yang W, Sanmamed MF, Badri T, Alawa J, López-Giráldez F, Gaule P, Lee SW, Zhang J-P-P, et al. PD-1H (Vista)-mediated suppression of autoimmunity in systemic and cutaneous lupus erythematosus. *Sci Transl Med*. 2019;11:1–15.
- Xu JL, Davis MM. Diversity in the CDR3 region of VH is sufficient for most antibody specificities. *Immunity*. 2000;13:37–45.
- van der Fits L, Mourits S, Voerman JSA, Kant M, Boon L, Laman JD, Cornelissen F, Mus A, Florencia E, Prens EP, et al. Imiquimod-induced psoriasis-like skin inflammation in mice is mediated via the IL-23/IL-17 axis. *J Immunol*. 2009;182:5836–45.
- Lin DY-W, Tanaka Y, Iwasaki M, Ag G, H-p S, Mikami B, Okazaki T, Honjo T, Minato N, Dn G. The PD-1/PD-L1 complex resembles the antigen-binding Fv domains of antibodies and T cell receptors. *Proc Natl Acad Sci*. 2008;105:3011–16.
- Tiegs G, Hentschel J, Wendel A. A T cell-dependent experimental liver injury in mice inducible by concanavalin A. *J Clin Invest*. 1992;90:196–203.
- Taniguchi T, Minami Y. The IL-2/IL-2 receptor system: a current overview. *Cell*. 1993;73:5–8.
- Taga K, Tosato G. IL-10 inhibits human T cell proliferation and IL-2 production. *J Immunol*. 1992;148:1143–48.
- ElTanbouly MA, Schaafsma E, Noelle RJ, Lines JL. Vista: coming of age as a multi-lineage immune checkpoint. *Clin Exp Immunol*. 2020;200:120–30.
- ElTanbouly MA, Zhao Y, Schaafsma E, Burns CM, Mabaera R, Cheng C, and Noelle RJ. Vista: a target to manage the innate cytokine storm. *Front Immunol*. 2021;11:595950.
- Kaneko Y, Nimmerjahn F, Ravetch JV. Anti-inflammatory activity of immunoglobulin G resulting from Fc sialylation. *Science* (80-). 2006;313:670–73.
- Abdallah MA, Abdel-Hamid MF, Kotb AM, Mabrouk EA. Serum interferon- $\gamma$  is a psoriasis severity and prognostic marker. *Cutis*. 2009;84:163–68.

24. Pietrzak AT, Zalewska A, Chodorowska G, Krasowska D, Michalak-Stoma A, Nockowski P, Osemlak P, Paszkowski T, Roliński JM. Cytokines and anticytokines in psoriasis. *Clin Chim Acta*. 2008;394:7–21.
25. Grine L, Steeland S, Van Ryckeghem S, Ballegeer M, Lienenklaus S, Weiss S, Sanders NN, Vandenbroucke RE, Libert C. Topical imiquimod yields systemic effects due to unintended oral uptake. *Sci Rep*. 2016;6:20134.
26. Zhang L. Type1 interferons potential initiating factors linking skin wounds with psoriasis pathogenesis. *Front Immunol*. 2019;10:1440.
27. Deng J, Li J, Sarde A, Lines JL, Lee Y-C-C, Qian DC, Pechenick DA, Manivanh R, Le Mercier I, Lowrey CH, et al. Hypoxia-induced Vista promotes the suppressive function of myeloid-derived suppressor cells in the tumor microenvironment. *Cancer Immunol Res*. 2019;7:1079–90.
28. Wang L, Jia B, Claxton DF, Ehmann WC, Rybka WB, Mineishi S, Naik S, Khawaja MR, Sivik J, Han J, et al. Vista is highly expressed on MDSCs and mediates an inhibition of T cell response in patients with AML. *Oncoimmunology*. 2018;7:e1469594.
29. Blando J, Sharma A, Higa MG, Zhao H, Vence L, Yadav SS, Kim J, Sepulveda AM, Sharp M, Maitra A, et al. Comparison of immune infiltrates in melanoma and pancreatic cancer highlights Vista as a potential target in pancreatic cancer. *Proc Natl Acad Sci*. 2019;116:1692–97.
30. Gao J, Ward JF, Pettaway CA, Shi LZ, Subudhi SK, Vence LM, Zhao H, Chen J, Chen H, Efstathiou E, et al. Vista is an inhibitory immune checkpoint that is increased after ipilimumab therapy in patients with prostate cancer. *Nat Med*. 2017;23:551–55.
31. Prodeus A, Abdul-Wahid A, Sparkes A, Fischer NW, Cydzik M, Chiang N, Alwash M, Ferzoco A, Vacaresse N, and Julius M, et al. Vista.COMP — an engineered checkpoint receptor agonist that potently suppresses T cell-mediated immune responses. *JCI Insight*. 2017;2(18):e94308.
32. Chardès T, Villard S, Ferrières G, Piechaczyk M, Cerutti M, Devauchelle G, Pau B. Efficient amplification and direct sequencing of mouse variable regions from any immunoglobulin gene family. *FEBS Lett*. 1999;452:386–94.
33. Sepulveda J, Shoemaker CB. Design and testing of PCR primers for the construction of scFv libraries representing the immunoglobulin repertoire of rats. *J Immunol Methods*. 2008;332:92–102.
34. Lefranc M-P, Pommié C, Ruiz M, Giudicelli V, Foulquier E, Truong L, Thouvenin-Contet V, Lefranc G. IMGT unique numbering for immunoglobulin and T cell receptor variable domains and Ig superfamily V-like domains. *Dev Comp Immunol*. 2003;27:55–77.
35. Ye J, Ma N, Madden TL, Ostell JM. IgBLAST: an immunoglobulin variable domain sequence analysis tool. *Nucleic Acids Res*. 2013;41:W34–40.
36. Sievers F, Wilm A, Dineen D, Tj G, Karplus K, Li W, Lopez R, McWilliam H, Remmert M, Söding J, et al. Fast, scalable generation of high-quality protein multiple sequence alignments using Clustal Omega. *Mol Syst Biol*. 2011;7:539.
37. Vincke C, Gutiérrez C, Wernery U, Devoogdt N, Hassanzadeh-Ghassabeh GMS. Generation of single domain antibody fragments derived from camelids and generation of manifold constructs. *Methods Mol Biol*. 2012;907:145–76.
38. Conrath KE, Lauwereys M, Galleni M, Matagne A, Frère JM, Kinne J, Wyns L, Muyldermans S.  $\beta$ -Lactamase inhibitors derived from single-domain antibody fragments elicited in the Camelidae. *Antimicrob Agents Chemother*. 2001;45:2807–12.
39. Romão E, Krasniqi A, Maes L, Vandenbrande C, Sterckx YG-J, Stijlemans B, Vincke C, Devoogdt N, Muyldermans S. Identification of nanobodies against the acute myeloid leukemia marker CD33. *Int J Mol Sci*. 2020;21:310.
40. Broussas M, Broyer L, and Goetsch L. . Evaluation of antibody-dependent cell cytotoxicity using lactate dehydrogenase (LDH) measurement. *Methods in molecular biology* 2013;988:305–17.